JCI insight

Intravascular hemolysis triggers ADP-mediated generation of platelet-rich thrombi in pre-capillary pulmonary arterioles

Tomasz Brzoska, … , Mark T. Gladwin, Prithu Sundd

JCI Insight. 2020. https://doi.org/10.1172/jci.insight.139437.

Research In-Press Preview **Pulmonology** **Vascular biology**

Patients with hereditary or acquired hemolytic anemias have a high risk of developing in-situ thrombosis of the pulmonary vasculature. While pulmonary thrombosis is a major morbidity associated with hemolytic disorders, the etiological mechanism underlying hemolysis-induced pulmonary thrombosis remains largely unknown. Here, we use intravital lung microscopy in mice for the first time to assess the pathogenesis of pulmonary thrombosis following deionized-water induced acute intravascular hemolysis. Acute hemolysis triggered the development of αIIbβ3-dependent platelet-rich thrombi in precapillary pulmonary arterioles, which led to the transient impairment of pulmonary blood flow. The hemolysis-induced pulmonary thrombosis was phenocopied with intravenous ADP- but not thrombin-triggered pulmonary thrombosis. Consistent with a mechanism involving ADP release from hemolyzing erythrocytes, the inhibition of platelet-$P2Y_{12}$ purinergic-receptor signaling attenuated pulmonary thrombosis and rescued blood flow in the pulmonary arterioles of mice following intravascular hemolysis. These findings are the first in vivo studies to suggest that acute intravascular hemolysis promotes ADP-dependent platelet activation leading to thrombosis in the pre-capillary pulmonary arterioles and that thrombin generation most likely does not play a significant role in the pathogenesis of acute hemolysis-triggered pulmonary thrombosis.

Title: Intravascular hemolysis triggers ADP-mediated generation of platelet-rich thrombi in pre-capillary pulmonary arterioles.

Authors: Tomasz Brzoska[1], Ravi Vats[1,2], Margaret F. Bennewitz[1,3], Egemen Tutuncuoglu[1], Simon C. Watkins[4], Margaret V. Ragni[5], Matthew D. Neal[6], Mark T. Gladwin[1,7], Prithu Sundd[1,2,7]*.

Affiliations:

1. Pittsburgh Heart, Lung and Blood Vascular Medicine Institute, University of Pittsburgh School of Medicine, Pittsburgh, PA, USA.
2. Department of Bioengineering, University of Pittsburgh, Pittsburgh, PA, USA.
3. Department of Chemical and Biomedical Engineering, West Virginia University, Morgantown, WV, USA.
4. Center for Biologic Imaging, University of Pittsburgh, Pittsburgh, PA, USA.
5. Department of Medicine, University of Pittsburgh, Hemophilia Center of Western Pennsylvania, Pittsburgh, PA, USA.
6. Department of Surgery, University of Pittsburgh School of Medicine, Pittsburgh, PA, USA.
7. Division of Pulmonary Allergy and Critical Care Medicine, University of Pittsburgh School of Medicine, Pittsburgh, PA, USA.

***To whom correspondence should be addressed:**
Prithu Sundd, PhD
Assistant Professor of Medicine
Division of Pulmonary, Allergy and Critical Care Medicine
Principal Investigator-Heart, Lung and Blood Vascular Medicine Institute
University of Pittsburgh School of Medicine
BST E1255, 200 Lothrop Street, Pittsburgh, PA 15261
E-mail: prs51@pitt.edu
Office: (412)-648-9103
Fax: (412)-648-5980

Running Head: Hemolysis triggers ADP-mediated lung thrombosis

Text word count: 3119

ABSTRACT

Patients with hereditary or acquired hemolytic anemias have a high risk of developing in-situ thrombosis of the pulmonary vasculature. While pulmonary thrombosis is a major morbidity associated with hemolytic disorders, the etiological mechanism underlying hemolysis-induced pulmonary thrombosis remains largely unknown. Here, we use intravital lung microscopy in mice for the first time to assess the pathogenesis of pulmonary thrombosis following deionized-water induced acute intravascular hemolysis. Acute hemolysis triggered the development of αIIbβ3-dependent platelet-rich thrombi in precapillary pulmonary arterioles, which led to the transient impairment of pulmonary blood flow. The hemolysis-induced pulmonary thrombosis was phenocopied with intravenous ADP- but not thrombin-triggered pulmonary thrombosis. Consistent with a mechanism involving ADP release from hemolyzing erythrocytes, the inhibition of platelet-$P2Y_{12}$ purinergic-receptor signaling attenuated pulmonary thrombosis and rescued blood flow in the pulmonary arterioles of mice following intravascular hemolysis. These findings are the first in vivo studies to suggest that acute intravascular hemolysis promotes ADP-dependent platelet activation leading to thrombosis in the pre-capillary pulmonary arterioles and that thrombin generation most likely does not play a significant role in the pathogenesis of acute hemolysis-triggered pulmonary thrombosis.

Abstract word count: 180

Key words: pulmonary thrombosis; platelets; purinergic signaling, intravital microscopy; pulmonary arterioles; hemolysis.

INTRODUCTION

Hemolysis is one of the major pathophysiological events associated with inherited and acquired disorders such as sickle cell disease (SCD) (1-3), thalassemia (1, 4), paroxysmal nocturnal hemoglobinuria (PNH) (5, 6), thrombotic thrombocytopenic purpura (TTP) (7, 8), hemolytic-uremic syndrome (HUS) (7, 9), sepsis (10, 11) and malaria (12). Intravascular hemolysis promotes the release of erythrocyte-derived damage associated molecular pattern molecules (eDAMPs), including cell free hemoglobin, heme, uric acid and adenosine diphosphate (ADP), that may directly and/or indirectly promote thrombosis, endothelial dysfunction and sterile inflammation (13-17). Although pulmonary thrombosis is a major clinical morbidity affecting patients with hemolytic disorders, how intravascular hemolysis promotes thrombosis in the lung remains poorly understood (18-26).

Hemolysis is associated with hemostatic abnormalities such as enhanced platelet activation and thrombin generation, elevated circulating tissue factor, and endothelial injury (1, 3, 5, 9, 15, 27-32). Thrombocytopenia, which is suggestive of intravascular platelet sequestration, is a risk factor for acute systemic and pulmonary complications of hemolytic disorders (8, 32-34). Importantly, autopsy and computed tomography studies have identified platelet-rich thrombi occluding pulmonary artery branches and arterioles in patients with diverse hemolytic disorders (19, 20, 25, 35, 36). Taken together, these findings suggest that in situ platelet aggregation within the pulmonary vasculature may potentially contribute to acute hemolysis-induced pulmonary thrombosis. However, the in vivo evidence and the molecular mechanism of this pathophysiology has remained elusive. Here, we use quantitative fluorescence intravital lung microscopy (qFILM) to reveal for the first time that acute intravascular (IV) hemolysis triggers pulmonary thrombosis

in mice, which is enabled by the occlusion of pre-capillary pulmonary arterioles by platelet-rich thrombi, leading to transient loss of blood flow in the lung. Our findings are the first in vivo studies to show that acute hemolysis-induced pulmonary thrombosis is largely mediated by ADP-dependent platelet-purinergic signaling, leading to platelet activation and αIIbβ3-dependent platelet aggregation in the pulmonary arterioles.

RESULTS

Intravascular hemolysis promotes platelet-dependent pulmonary arteriole thrombosis

QFILM revealed absence of pulmonary thrombosis in mice IV administered saline (control mice). In control mice, blood (purple fluorescence) was observed to flow unobstructed through the pulmonary vasculature with erythrocytes visible as rapidly transiting dark cells (Supplemental Figure 1 and Supplemental Video 1). Previously, IV administration of deionized water (dH_2O) has been shown to trigger acute intravascular hemolysis in mice in vivo (37). QFILM revealed that IV administration of dH_2O triggered the development of platelet-rich thrombi (green fluorescence) in the pre-capillary pulmonary arterioles of mice (Figure 1, Supplemental Video 2). As shown in Supplemental Video 2, these thrombi were primarily formed in the pulmonary arteriolar bottle-necks (junction of pulmonary arteriole and capillaries) and resolved entirely over the next ~2 min, resulting in a transient impairment of pulmonary blood flow. The time-series of qFILM images were analyzed over several mice to determine the kinetics of pulmonary thrombosis in terms of three separate parameters: total pulmonary thrombi area as a function of time (Figure 1B), max pulmonary thrombi area (red arrow in Figure 1B) and area under the curve (AUC, later shown in Figure 2D) as described in Methods. Next, we used eptifibatide, which is an antagonist of platelet receptor αIIbβ3 (38) and FDA approved drug for the prevention of platelet aggregation-dependent thrombosis in broad range of ischemic coronary conditions including percutaneous coronary intervention, acute coronary syndrome and unstable angina (38). Remarkably, pretreatment with 10 mg/kg IV eptifibatide completely abrogated IV dH_2O triggered pulmonary thrombosis in mice (Figure 2A-B, Supplemental Video 3), which was evident by the significant reduction in both pulmonary thrombi max area (Figure 2B, C) and AUC (Figure 2D). These findings indicate that

pulmonary arteriole thrombosis triggered by acute intravascular hemolysis is predominantly dependent on platelet activation and subsequent aggregation.

Acute hemolysis-induced pulmonary thrombosis is unlikely to be thrombin-dependent

Thrombin directly activates a number of coagulation factors, cleaves fibrinogen to fibrin and stimulates protease activated receptors (PARs) on platelets to promote thrombosis (39, 40). Importantly, markers of thrombin generation such as, prothrombin fragment F1 + 2, thrombin-antithrombin III complexes and D-dimers have been found to be significantly elevated in diverse hemolytic disorders (9, 41-45). Therefore, we compared the pathophysiology of pulmonary thrombosis triggered by IV dH_2O (acute hemolysis) to the one by IV thrombin. Unlike the transient pulmonary thrombosis triggered by acute hemolysis (Figure 1), mice challenged with 250 U/kg IV thrombin developed protracted pulmonary thrombosis accompanied by the development of platelet-rich thrombi within the pulmonary arteriolar bottlenecks (Figure 3A, C and Supplemental Video 4). Subsequently, we examined the effect of 500 U/kg IV thrombin on the pulmonary thrombosis development in mice. Seventy five percent of mice challenged with higher dose of 500 U/kg IV thrombin died, which was also accompanied by the loss of the pulmonary blood flow (Figure 3B, D, E and Supplemental Video 5). Unexpectedly, the average pulmonary thrombi max area in mice administered 500 U/kg IV thrombin was not significantly higher than mice administered 250 U/kg IV thrombin (Figure 3F), which was probably caused by the pulmonary thrombosis in large arterial branches (>50 μm) upstream of pulmonary arterioles in mice administered 500 U/kg IV thrombin (Figure 3G, Supplemental Video 6). In contrast to the effect of eptifibatide on hemolysis-induced pulmonary thrombosis (Figure 2), eptifibatide failed to prevent severe pulmonary thrombosis (Figure 4A-B, Supplemental Video 7) and lethality (Figure

4C) following IV administration of 500 U/kg thrombin. The mean pulmonary-thrombi-max-area in mice treated with eptifibatide prior to 500 U/kg IV thrombin was not different from mice treated with 500 U/kg IV thrombin only (Supplemental Figure 2), further suggesting that eptifibatide did not attenuate thrombin-triggered pulmonary arteriole thrombosis in mice. This difference in the pathophysiology of acute hemolysis vs IV thrombin induced pulmonary thrombosis suggest that thrombin generation most likely does not play a significant role in the pathogenesis of acute hemolysis-triggered pulmonary thrombosis.

Acute hemolysis-induced pulmonary thrombosis is likely to be ADP-dependent

Intravascular hemolysis is also known to promote the release of ADP from erythrocytes (46-48), which can bind to $P2Y_1$ and $P2Y_{12}$ purinergic receptors on platelets to trigger platelet activation and subsequent aggregation (49, 50). Therefore, we next compared the pathophysiology of pulmonary thrombosis triggered by acute hemolysis to the one by IV administration of ADP. Similar to acute hemolysis (Figure 1), IV ADP led to the development of transient pulmonary thrombosis in mice in a dose-dependent manner (Figure 5). Mice treated with 0.5 mg/kg IV ADP manifested mild pulmonary thrombosis (Supplemental Figure 3 and Supplemental Video 8), while, IV administration of 2.5 mg/kg ADP led to the development of medium (500-1000 μm^2) and large (>1000 μm^2) platelet-rich thrombi (green fluorescence) in the pulmonary arterioles (Figure 5A and Supplemental Video 9). Identical to acute hemolysis-induced pulmonary thrombosis (Figure 1), IV ADP-induced thrombi were initially unable to pass through the arteriolar bottlenecks causing transient obstruction of the blood flow. As shown in Supplemental Video 9, the occlusion of arteriolar bottlenecks by platelet-rich thrombi resulted in transient ischemia evident by the gradual loss of the vascular dye (purple fluorescence) in the capillaries downstream of occluded arteriole,

followed by resolution of pulmonary thrombosis and complete recovery of blood flow (rescue of purple fluorescence) within 5 min after IV ADP. The total pulmonary thrombi area (Figure 5D), mean pulmonary thrombi max area (Figure 5E) and AUC (Figure 5F) were significantly larger following administration of 2.5 than 0.5 mg/kg IV ADP. Identical to the effect of eptifibatide on hemolysis-induced pulmonary thrombosis (Figure 2), 10 mg/kg IV eptifibatide completely abrogated ADP-induced pulmonary thrombosis in mice (Figure 6). In contrast, heparin, a potent anticoagulant (51) was ineffective in preventing IV ADP induced transient pulmonary thrombosis in mice (Supplemental Figure 4A-B, Supplemental Video 10). Both, the mean pulmonary thrombi max area and the AUC were significantly attenuated by eptifibatide (Figure 6B-D) but not heparin (Supplemental Figure 4B-D) in mice IV administered ADP. As shown in Supplemental Figure 5, the pulmonary thrombi max area was not significantly different between IV dH2O and 0.5 mg/kg IV ADP challenged mice. The similarities in the pathophysiology of acute hemolysis and IV ADP induced pulmonary thrombosis suggest that ADP released from lysed erythrocytes most likely plays a major role in the pathogenesis of acute hemolysis-triggered pulmonary thrombosis.

ADP-activates platelet $P2Y_{12}$ receptor to promote hemolysis-induced pulmonary thrombosis

Next, we tested whether inhibiting ADP-dependent platelet activation prevents acute hemolysis induced pulmonary thrombosis in mice. Prasugrel is a thienopyridine class of drug, which is used clinically to treat patients with acute coronary syndrome who are undergoing percutaneous coronary intervention (52, 53). When taken orally, the active metabolite of prasugrel acts as a selective, irreversible and potent platelet $P2Y_{12}$ receptor antagonist, and prevents ADP-dependent platelet activation (54). We pretreated mice with 3 or 10 mg/kg prasugrel by oral gavage (PO) for two days and prior to inducing acute intravascular hemolysis by IV administering dH_2O (refer to

Methods). Remarkably, prasugrel pretreatment inhibited acute-hemolysis induced pulmonary arteriole thrombosis in a dose-dependent manner (Figure 7 and Supplemental Figure 6). Prasugrel inhibited both the formation and subsequent sequestration of platelet-rich thrombi in the pulmonary arterioles (Figure 7A-B, Supplemental Figure 6A-B, Supplemental Videos 11 and 12). The pulmonary thrombi max area (Figure 7B-C, Supplemental Figure 6B-C) and AUC (Figure 7D) were significantly attenuated in mice treated with prasugrel prior to IV dH_2O. As shown in Supplemental Videos 11 and 12, mice pretreated with prasugrel prior to IV dH_2O did not develop medium and large platelet-rich thrombi (>500 μm^2) observed in IV dH_2O administered mice (Figure 1 and Supplemental Video 2). Although small platelet-rich thrombi (<500 μm^2) were still observed in the pulmonary arterioles of prasugrel treated mice, these thrombi were too small to obstruct the pulmonary blood flow (Figure 7A; Supplemental Figure 6A; Supplemental Videos 11 and 12). These findings suggest that ADP-dependent platelet $P2Y_{12}$ signaling plays a major role in acute hemolysis-induced pulmonary arteriole thrombosis.

DISCUSSION

Epidemiological evidence suggests that in situ pulmonary thrombosis is a major pathological event contributing to cardiopulmonary morbidities associated with hemolytic disorders, however, the molecular, cellular and biophysical mechanisms of hemolysis-induced pulmonary thrombosis remains incompletely understood (19, 20, 35, 36). To address this, we have used intravital microscopy to study the kinetics of pulmonary thrombosis progression in mice, following acute intravascular hemolysis (IV dH_2O). Acute hemolysis led to transient pulmonary thrombosis in mice in vivo, which was caused by the development of platelet-rich thrombi in the precapillary pulmonary arterioles, leading to impairment of pulmonary blood flow.

We found that acute intravascular hemolysis led to transient non-lethal pulmonary arteriole thrombosis in mice, which was dependent on αIIbβ3-mediated platelet aggregation. Previous studies suggest that ADP released from lysed erythrocytes may play a role in platelet activation (47, 55). Although ADP is known to activate platelet-purinergic receptors $P2Y_1$ and $P2Y_{12}$ to induce platelet shape change, degranulation and reversible aggregation in vitro (56), a role for ADP-dependent purinergic signaling in hemolysis-induced pulmonary thrombosis in vivo has never been reported. We show for the first time that pulmonary thrombosis triggered by acute hemolysis, shares pathogenesis with ADP but not thrombin-triggered pulmonary thrombosis in mice in vivo. We also show for the first time that acute hemolysis-induced pulmonary thrombosis is abolished following the inhibition of platelet-$P2Y_{12}$-receptor signaling. Taken together, these findings suggest that ADP released during acute hemolysis activates purinergic signaling in platelets to promote αIIbβ3-dependent acute reversible pulmonary arteriole thrombosis.

Our current study has few limitations that need to be addressed in future investigations. First, the current study investigates the mechanism of pulmonary thrombosis secondary to acute intravascular hemolysis. Importantly, low-grade chronic hemolysis also occurs in several hemolytic disorders (1, 5, 8, 10, 15), and could possibly have additional implications on pulmonary thrombosis that did not manifest in our acute hemolysis model. Second, anionic phospholipids exposed on lysed-erythrocyte membrane fragments also promote coagulation and therefore, may contribute to hemolysis-induced pulmonary thrombosis (1, 42). Third, von Willebrand factor (VWF) released by injured endothelium may also contribute to pulmonary thrombosis, by promoting platelet adhesion and activation (57). Indeed, platelet interaction with VWF has been shown to play a crucial role in the pathophysiology of multiple hemolytic disorders including TTP (7, 8, 20, 58). Fourth, nitric oxide (NO) depletion and reactive oxygen species (ROS) generation by cell-free hemoglobin may also contribute to hemolysis-induced platelet activation and pulmonary thrombosis (3, 17, 27, 55). Fifth, although thrombin did not seem to play a direct role in our study, thrombin generation may still contribute to acute hemolysis-triggered pulmonary thrombosis by unknown mechanisms. Sixth, changes in the vascular tone caused by thrombin or adenosine generated during hemolysis, may regulate the pathogenesis of acute hemolysis-induced pulmonary thrombosis. Notwithstanding these limitations, the current study is the first to use intravital lung microscopy in live mice to reveal that platelet-purinergic signaling promotes platelet-dependent pulmonary arteriole thrombosis associated with acute intravascular hemolysis.

METHODS

Reagents, animals and surgical preparation

Wild type C57BL/6J mice (8-12 weeks old) were purchased from Jackson Laboratory. See online supplement for details on used reagents and mouse surgical preparation.

Quantitative fluorescence intravital lung microscopy (qFILM) of pulmonary thrombosis

The current study is an adaptation of qFILM approach used previously (59-63). QFILM of the mouse pulmonary microcirculation was performed using a Nikon A1R Multi-Photon-Excitation (MPE) Ni-E upright motorized microscope (Nikon Instruments; Tokyo, Japan). Two-dimensional time series of qFILM images were acquired with NIS-Elements software using a prechirped Chameleon Laser Vision (Coherent; Santa Clara, CA) emitting an excitation wavelength of 850 nm, an APO LWD 25x water immersion objective with 1.1 NA, a high-speed resonant scanning mode capable of acquisition at 512 x 512 resolution with 2x line averaging and bi-directional scanning (~15 frames per second) and four GaAsP NDD detectors. The four detectors collected fluorescent light transmitted through 450/20 nm (detector 1; blue channel), 525/50 nm (detector 2; green channel), 576/26 nm (detector 3; red channel) and 685/70 nm (detector 4; far red channel) band pass filters. In this study, we used detector 1 for V450 and detector 2 for FITC. The position of the microscope stage was selected in the z and x-y planes through a Nano-Drive (Mad City Labs Inc.; Madison, WI) and a control pad (Prior Scientific Inc.; Rockland, MA), respectively. A single 2D plane (FOV ~512 pixel x 512 pixel at 0.67 μm per pixel resolution) in the z-direction was selected and multiple images were acquired at a rate of 15 frames/s for each mouse. Hemolysis in mice was evoked by intravascular (IV) injection of deionized water (dH_2O 150 μl) through a

catheter placed in carotid artery (37). IV dH_2O (150 µl) is known to trigger a physiologically relevant level of acute hemolysis in mice (37, 64, 65). Pulmonary thrombosis was also induced in mice by IV administration of adenosine diphosphate (ADP) or thrombin. Some mice were given IV heparin (300 U/kg) or eptifibatide (10 mg/kg) 15 minutes before initiation of pulmonary thrombosis (66, 67). Prasugrel was suspended in a 5% solution of gum arabic (68) and administered once a day for 2 days and additionally approximately 4 hours before qFILM to each mouse by oral gavage (PO) with a volume of 10 ml/kg. Physiological saline was IV administered to mice as a vehicle in control experiments. FITC-dextran (75 µg/mouse) and V450-conjugated anti-CD49b mAb (7 µg/mouse) were IV administered through the carotid artery catheter to enable in vivo visualization of the lung microcirculation and in vivo staining of platelets, respectively. Anti-CD49b mAb has been used widely for in vivo visualization of platelets.(60, 69, 70) In each mouse, a single field of view (FOV~118000 μm^2) containing a pulmonary arteriole (30 to 50 µm diameter) and the downstream pulmonary capillary bed was randomly selected and presence or absence of pulmonary thrombosis was assessed using qFILM. These assessments were conducted in 3 to 7 mice in each test group. Time-series of qFILM images of pulmonary arteriolar microcirculation in each FOV was recorded prior (t = 0 sec) and up to 30 min after IV administration of dH_2O, ADP or thrombin, followed by euthanization of mouse with an overdose of anesthesia.

QFILM image processing and data analysis

Refer to online supplement for details on qFILM image processing. Pulmonary arterioles and downstream capillaries were analyzed for the quantitative assessment of pulmonary thrombosis. Arterioles were identified as blood vessels draining blood into smaller daughter arterioles followed

by even smaller pulmonary capillaries. Platelet-rich pulmonary thrombi were defined as platelet aggregates (area > 10 μm^2) sequestered within the pre-capillary pulmonary arterioles and extending down into the pulmonary capillaries. Two-dimensional sizes (areas in μm^2) of platelet-rich thrombi were estimated in NIS-Elements software (NIKON, USA) by converting qFILM images into binary images and adjusting the threshold range of the intensity histograms uniformly over the entire FOV in each image frame of the time-series (Supplemental Figure 7). The sizes of all the platelet-rich thrombi in a single image frame were added to generate total pulmonary thrombi area, which was plotted as a function of time in GraphPad Prism 7 (GraphPad Software; La Jolla, CA). This approach allowed us to follow the kinetic of initiation and progression of pulmonary thrombosis in observed FOV. Changes in total pulmonary thrombi area over time served to calculate pulmonary thrombi maximum area (Pulmonary thrombi max area) and area under the curve (AUC). Pulmonary thrombi max area value reflects the maximum total area of platelet-rich thrombi in a FOV during the qFILM observation period. AUC is a combined measure of both size and lifetime of platelet-rich thrombi during the qFILM observation period. In some experiments, development of pulmonary thrombosis resulted in irreversible cessation of pulmonary blood flow, followed by mouse death. For such experiments, AUC was not estimated.

Statistics

Pulmonary thrombi max area and AUC were compared between groups using the Wilcoxon-Mann-Whitney test (when the data was not normally distributed) or the two-tailed unpaired Student's t test (when the data was normally distributed). Survival data were compared using Kaplan–Meier log rank (Mantel–Cox) test. Error bars in dot plots represent mean ± standard error (SE). P-value of less than 0.05 was used to determine significance.

Study approval

All animal experiments were approved by the Institutional Animal Care and Use Committee of the University of Pittsburgh.

Author's contributions: TB designed, performed, analyzed the qFILM experiments and wrote the manuscript. RV, MFB and SCW contributed to the qFILM experiments. ET was responsible for mouse colony management. MVR, MDN and MTG were involved in experimental design and manuscript writing. PS was responsible for experimental design, manuscript writing, and project supervision. TB and PS wrote the manuscript with consultation and contribution from all coauthors.

Conflict-of-interest disclosure: The authors declare no competing financial interests.

Funding: This study was supported by NHLBI 1R01HL128297-01 (PS), NHLBI 1R01 HL141080-01A1 (PS and MDN), 1R35GM119526-01 (MDN), American Heart Association 18TPA34170588 (PS), funds from the Hemophilia Center of Western Pennsylvania and Vitalant (PS), American Society of Hematology Postdoctoral Scholar Award (TB) and American Heart Association predoctoral fellowship 19PRE34430188 (RV). The Nikon multiphoton excitation microscope was funded by NIH grants 1S10RR028478-01 and S10OD025041 (SCW).

References

1. Ataga KI, Cappellini MD, and Rachmilewitz EA. Beta-thalassaemia and sickle cell anaemia as paradigms of hypercoagulability. *Br J Haematol.* 2007;139(1):3-13.
2. Ataga KI, and Key NS. Hypercoagulability in sickle cell disease: new approaches to an old problem. *Hematology Am Soc Hematol Educ Program.* 2007:91-6.
3. Brzoska T, Kato GJ, and Sundd P. In: Michelson AD ed. *Platelets*. Elsevier Inc.; 2019:563-80.
4. Eldor A, and Rachmilewitz EA. The hypercoagulable state in thalassemia. *Blood.* 2002;99(1):36-43.
5. Van Bijnen ST, Van Heerde WL, and Muus P. Mechanisms and clinical implications of thrombosis in paroxysmal nocturnal hemoglobinuria. *J Thromb Haemost.* 2012;10(1):1-10.
6. de Latour RP, Mary JY, Salanoubat C, Terriou L, Etienne G, Mohty M, et al. Paroxysmal nocturnal hemoglobinuria: natural history of disease subcategories. *Blood.* 2008;112(8):3099-106.
7. George JN, and Nester CM. Syndromes of thrombotic microangiopathy. *N Engl J Med.* 2014;371(7):654-66.
8. Joly BS, Coppo P, and Veyradier A. Thrombotic thrombocytopenic purpura. *Blood.* 2017;129(21):2836-46.
9. Chandler WL, Jelacic S, Boster DR, Ciol MA, Williams GD, Watkins SL, et al. Prothrombotic coagulation abnormalities preceding the hemolytic-uremic syndrome. *N Engl J Med.* 2002;346(1):23-32.

10. Effenberger-Neidnicht K, and Hartmann M. Mechanisms of Hemolysis During Sepsis. *Inflammation.* 2018;41(5):1569-81.

11. Semeraro N, Ammollo CT, Semeraro F, and Colucci M. Sepsis, thrombosis and organ dysfunction. *Thromb Res.* 2012;129(3):290-5.

12. Cunnington AJ, Njie M, Correa S, Takem EN, Riley EM, and Walther M. Prolonged neutrophil dysfunction after Plasmodium falciparum malaria is related to hemolysis and heme oxygenase-1 induction. *J Immunol.* 2012;189(11):5336-46.

13. Gladwin MT, and Ofori-Acquah SF. Erythroid DAMPs drive inflammation in SCD. *Blood.* 2014;123(24):3689-90.

14. Kato GJ, Steinberg MH, and Gladwin MT. Intravascular hemolysis and the pathophysiology of sickle cell disease. *J Clin Invest.* 2017;127(3):750-60.

15. Ataga KI. Hypercoagulability and thrombotic complications in hemolytic anemias. *Haematologica.* 2009;94(11):1481-4.

16. Rother RP, Bell L, Hillmen P, and Gladwin MT. The clinical sequelae of intravascular hemolysis and extracellular plasma hemoglobin: a novel mechanism of human disease. *JAMA.* 2005;293(13):1653-62.

17. Sundd P, Gladwin MT, and Novelli EM. Pathophysiology of Sickle Cell Disease. *Annu Rev Pathol.* 2019;14:263-92.

18. Adedeji MO, Cespedes J, Allen K, Subramony C, and Hughson MD. Pulmonary thrombotic arteriopathy in patients with sickle cell disease. *Arch Pathol Lab Med.* 2001;125(11):1436-41.

19. Mekontso Dessap A, Deux JF, Abidi N, Lavenu-Bombled C, Melica G, Renaud B, et al. Pulmonary artery thrombosis during acute chest syndrome in sickle cell disease. *Am J Respir Crit Care Med.* 2011;184(9):1022-9.

20. Anea CB, Lyon M, Lee IA, Gonzales JN, Adeyemi A, Falls G, et al. Pulmonary platelet thrombi and vascular pathology in acute chest syndrome in patients with sickle cell disease. *Am J Hematol.* 2016;91(2):173-8.

21. Sonakul D, Pacharee P, Laohapand T, Fucharoen S, and Wasi P. Pulmonary artery obstruction in thalassaemia. *Southeast Asian J Trop Med Public Health.* 1980;11(4):516-23.

22. Hill A, Sapsford RJ, Scally A, Kelly R, Richards SJ, Khurisgara G, et al. Under-recognized complications in patients with paroxysmal nocturnal haemoglobinuria: raised pulmonary pressure and reduced right ventricular function. *Br J Haematol.* 2012;158(3):409-14.

23. Panoskaltsis N, Derman MP, Perillo I, and Brennan JK. Thrombotic thrombocytopenic purpura in pulmonary-renal syndromes. *Am J Hematol.* 2000;65(1):50-5.

24. Martinez AJ, Maltby JD, and Hurst DJ. Thrombotic thrombocytopenic purpura seen as pulmonary hemorrhage. *Arch Intern Med.* 1983;143(9):1818-20.

25. Upadhyaya K, Barwick K, Fishaut M, Kashgarian M, and Siegel NJ. The importance of nonrenal involvement in hemolytic-uremic syndrome. *Pediatrics.* 1980;65(1):115-20.

26. Blaisdell FW. Pathophysiology of the respiratory distress syndrome. *Arch Surg.* 1974;108(1):44-9.

27. Villagra J, Shiva S, Hunter LA, Machado RF, Gladwin MT, and Kato GJ. Platelet activation in patients with sickle disease, hemolysis-associated pulmonary hypertension, and nitric oxide scavenging by cell-free hemoglobin. *Blood.* 2007;110(6):2166-72.

28. Polanowska-Grabowska R, Wallace K, Field JJ, Chen L, Marshall MA, Figler R, et al. P-selectin-mediated platelet-neutrophil aggregate formation activates neutrophils in mouse and human sickle cell disease. *Arterioscler Thromb Vasc Biol.* 2010;30(12):2392-9.

29. Eldor A, Lellouche F, Goldfarb A, Rachmilewitz EA, and Maclouf J. In vivo platelet activation in beta-thalassemia major reflected by increased platelet-thromboxane urinary metabolites. *Blood.* 1991;77(8):1749-53.

30. Ruf A, Pick M, Deutsch V, Patscheke H, Goldfarb A, Rachmilewitz EA, et al. In-vivo platelet activation correlates with red cell anionic phospholipid exposure in patients with beta-thalassaemia major. *Br J Haematol.* 1997;98(1):51-6.

31. Wiedmer T, Hall SE, Ortel TL, Kane WH, Rosse WF, and Sims PJ. Complement-induced vesiculation and exposure of membrane prothrombinase sites in platelets of paroxysmal nocturnal hemoglobinuria. *Blood.* 1993;82(4):1192-6.

32. Karpman D, Manea M, Vaziri-Sani F, Stahl AL, and Kristoffersson AC. Platelet activation in hemolytic uremic syndrome. *Semin Thromb Hemost.* 2006;32(2):128-45.

33. Chaturvedi S, Ghafuri DL, Glassberg J, Kassim AA, Rodeghier M, and DeBaun MR. Rapidly progressive acute chest syndrome in individuals with sickle cell anemia: a distinct acute chest syndrome phenotype. *Am J Hematol.* 2016;91(12):1185-90.

34. Alhandalous CH, Han J, Hsu L, Gowhari M, Hassan J, Molokie R, et al. Platelets decline during Vaso-occlusive crisis as a predictor of acute chest syndrome in sickle cell disease. *Am J Hematol.* 2015;90(12):E228-9.

35. Sumiyoshi A, Thakerngpol K, and Sonakul D. Pulmonary microthromboemboli in thalassemic cases. *Southeast Asian J Trop Med Public Health.* 1992;23 Suppl 2:29-31.

36. Nokes T, George JN, Vesely SK, and Awab A. Pulmonary involvement in patients with thrombotic thrombocytopenic purpura. *Eur J Haematol.* 2014;92(2):156-63.

37. Almeida CB, Souza LE, Leonardo FC, Costa FT, Werneck CC, Covas DT, et al. Acute hemolytic vascular inflammatory processes are prevented by nitric oxide replacement or a single dose of hydroxyurea. *Blood.* 2015;126(6):711-20.

38. O'Shea JC, and Tcheng JE. Eptifibatide: a potent inhibitor of the platelet receptor integrin glycoprotein IIb/IIIa. *Expert Opin Pharmacother.* 2002;3(8):1199-210.

39. Hoffman M, and Monroe DM, 3rd. A cell-based model of hemostasis. *Thromb Haemost.* 2001;85(6):958-65.

40. Wolberg AS, Rosendaal FR, Weitz JI, Jaffer IH, Agnelli G, Baglin T, et al. Venous thrombosis. *Nat Rev Dis Primers.* 2015;1:15006.

41. Peters M, Plaat BE, ten Cate H, Wolters HJ, Weening RS, and Brandjes DP. Enhanced thrombin generation in children with sickle cell disease. *Thromb Haemost.* 1994;71(2):169-72.

42. Tomer A, Harker LA, Kasey S, and Eckman JR. Thrombogenesis in sickle cell disease. *J Lab Clin Med.* 2001;137(6):398-407.

43. Francis RB, Jr. Elevated fibrin D-dimer fragment in sickle cell anemia: evidence for activation of coagulation during the steady state as well as in painful crisis. *Haemostasis.* 1989;19(2):105-11.

44. Kurantsin-Mills J, Ofosu FA, Safa TK, Siegel RS, and Lessin LS. Plasma factor VII and thrombin-antithrombin III levels indicate increased tissue factor activity in sickle cell patients. *Br J Haematol.* 1992;81(4):539-44.

45. Cappellini MD, Robbiolo L, Bottasso BM, Coppola R, Fiorelli G, and Mannucci AP. Venous thromboembolism and hypercoagulability in splenectomized patients with thalassaemia intermedia. *Br J Haematol.* 2000;111(2):467-73.

46. Born GV, Bergquist D, and Arfors KE. Evidence for inhibition of platelet activation in blood by a drug effect on erythrocytes. *Nature.* 1976;259(5540):233-5.

47. Gaarder A, Jonsen J, Laland S, Hellem A, and Owren PA. Adenosine diphosphate in red cells as a factor in the adhesiveness of human blood platelets. *Nature.* 1961;192:531-2.

48. Eltzschig HK, Sitkovsky MV, and Robson SC. Purinergic signaling during inflammation. *N Engl J Med.* 2012;367(24):2322-33.

49. Jin J, and Kunapuli SP. Coactivation of two different G protein-coupled receptors is essential for ADP-induced platelet aggregation. *Proc Natl Acad Sci U S A.* 1998;95(14):8070-4.

50. Holmsen H, and Weiss HJ. Secretable storage pools in platelets. *Annu Rev Med.* 1979;30:119-34.

51. Rosenberg RD. Actions and interactions of antithrombin and heparin. *N Engl J Med.* 1975;292(3):146-51.

52. Jakubowski JA, Winters KJ, Naganuma H, and Wallentin L. Prasugrel: a novel thienopyridine antiplatelet agent. A review of preclinical and clinical studies and the mechanistic basis for its distinct antiplatelet profile. *Cardiovasc Drug Rev.* 2007;25(4):357-74.

53. Wright RS, Anderson JL, Adams CD, Bridges CR, Casey DE, Jr., Ettinger SM, et al. 2011 ACCF/AHA focused update incorporated into the ACC/AHA 2007 Guidelines for the Management of Patients with Unstable Angina/Non-ST-Elevation Myocardial Infarction:

a report of the American College of Cardiology Foundation/American Heart Association Task Force on Practice Guidelines developed in collaboration with the American Academy of Family Physicians, Society for Cardiovascular Angiography and Interventions, and the Society of Thoracic Surgeons. *J Am Coll Cardiol.* 2011;57(19):e215-367.

54. Niitsu Y, Jakubowski JA, Sugidachi A, and Asai F. Pharmacology of CS-747 (prasugrel, LY640315), a novel, potent antiplatelet agent with in vivo P2Y12 receptor antagonist activity. *Semin Thromb Hemost.* 2005;31(2):184-94.

55. Helms CC, Marvel M, Zhao W, Stahle M, Vest R, Kato GJ, et al. Mechanisms of hemolysis-associated platelet activation. *J Thromb Haemost.* 2013;11(12):2148-54.

56. Remijn JA, Wu YP, Jeninga EH, MJ IJ, van Willigen G, de Groot PG, et al. Role of ADP receptor P2Y(12) in platelet adhesion and thrombus formation in flowing blood. *Arterioscler Thromb Vasc Biol.* 2002;22(4):686-91.

57. Chen J, and Lopez JA. Interactions of platelets with subendothelium and endothelium. *Microcirculation.* 2005;12(3):235-46.

58. Krishnan S, Siegel J, Pullen G, Jr., Hevelow M, Dampier C, and Stuart M. Increased von Willebrand factor antigen and high molecular weight multimers in sickle cell disease associated with nocturnal hypoxemia. *Thromb Res.* 2008;122(4):455-8.

59. Bennewitz MF, Watkins SC, and Sundd P. Quantitative intravital two-photon excitation microscopy reveals absence of pulmonary vaso-occlusion in unchallenged Sickle Cell Disease mice. *Intravital.* 2014;3(2):e29748.

60. Bennewitz MF, Jimenez MA, Vats R, Tutuncuoglu E, Jonassaint J, Kato GJ, et al. Lung vaso-occlusion in sickle cell disease mediated by arteriolar neutrophil-platelet microemboli. *JCI Insight.* 2017;2(1):e89761.

61. Bennewitz MF, Tutuncuoglu E, Gudapati S, Brzoska T, Watkins SC, Monga SP, et al. P-selectin-deficient mice to study pathophysiology of sickle cell disease. *Blood Adv.* 2020;4(2):266-73.

62. Sparkenbaugh EM, Chen C, Brzoska T, Nguyen J, Wang S, Vercellotti GM, et al. Thrombin-mediated activation of PAR-1 contributes to microvascular stasis in mouse models of sickle cell disease. *Blood.* 2020.

63. Vats R, Brzoska T, Bennewitz MF, Jimenez MA, Pradhan-Sundd T, Tutuncuoglu E, et al. Platelet Extracellular Vesicles Drive Inflammasome-IL-1beta-Dependent Lung Injury in Sickle Cell Disease. *Am J Respir Crit Care Med.* 2020;201(1):33-46.

64. Wajih N, Basu S, Jailwala A, Kim HW, Ostrowski D, Perlegas A, et al. Potential therapeutic action of nitrite in sickle cell disease. *Redox Biol.* 2017;12:1026-39.

65. Conran N, and Almeida CB. Hemolytic vascular inflammation: an update. *Rev Bras Hematol Hemoter.* 2016;38(1):55-7.

66. Atkinson BT, Jasuja R, Chen VM, Nandivada P, Furie B, and Furie BC. Laser-induced endothelial cell activation supports fibrin formation. *Blood.* 2010;116(22):4675-83.

67. Araki H, Nishi K, Ishihara N, and Okajima K. Inhibitory effects of activated protein C and heparin on thrombotic arterial occlusion in rat mesenteric arteries. *Thromb Res.* 1991;62(3):209-16.

68. Ohno K, Tomizawa A, Mizuno M, Jakubowski JA, and Sugidachi A. Prasugrel, a Platelet P2Y12 Receptor Antagonist, Improves Abnormal Gait in a Novel Murine Model of Thrombotic Hindlimb Ischemia. *J Am Heart Assoc.* 2016;5(4):e002889.

69. Wong CH, Jenne CN, Petri B, Chrobok NL, and Kubes P. Nucleation of platelets with blood-borne pathogens on Kupffer cells precedes other innate immunity and contributes to bacterial clearance. *Nat Immunol.* 2013;14(8):785-92.

70. Vats R, Brzoska T, Bennewitz MF, Jimenez MA, Pradhan-Sundd T, Tutuncuoglu E, et al. Platelet Extracellular Vesicles Drive Inflammasome-IL1beta-dependent Lung Injury in Sickle Cell Disease. *Am J Respir Crit Care Med.* 2019.

Figure 1

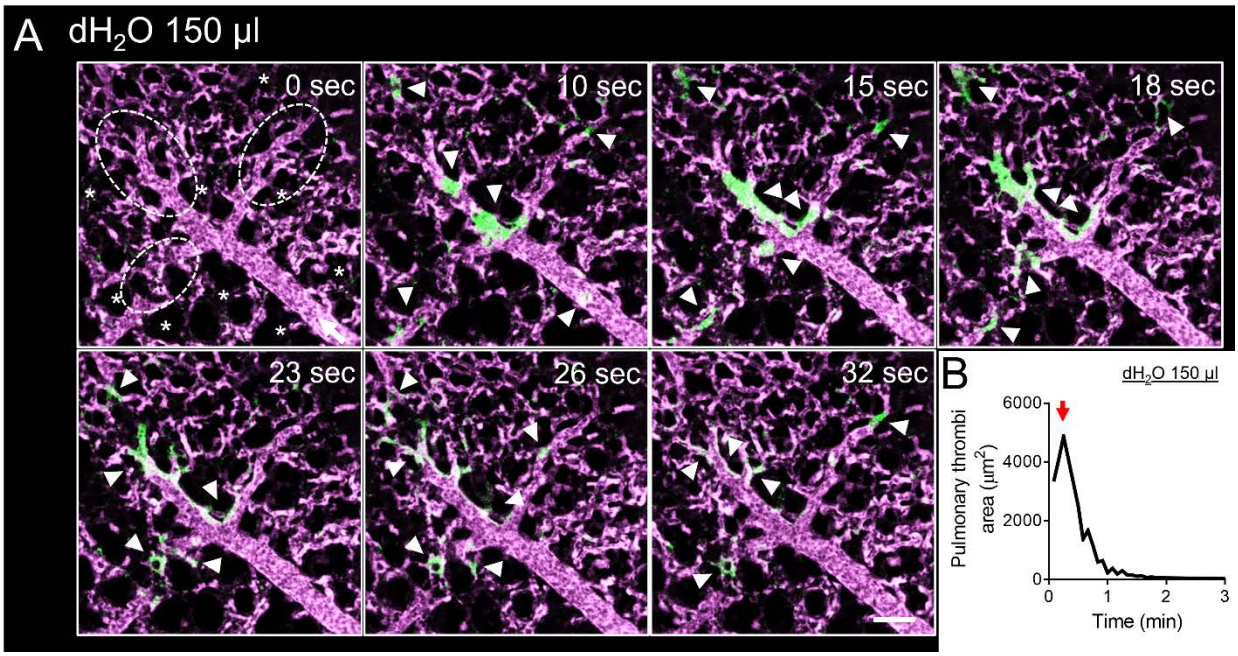

Figure 1. Intravascular hemolysis triggers acute pulmonary thrombosis in mice. WT mice were intravascularly (IV) administered with 150 µl dH_2O (n = 7 mice) to induce acute hemolysis and pulmonary circulation was imaged using quantitative fluorescence intravital lung microscopy (qFILM). **(A)** qFILM images of the same field of view (FOV) at 7 different time points are shown. t = 0 s corresponds to time point before IV dH_2O administration and other displayed time points are relative to IV dH_2O. Pulmonary thrombosis was absent at t = 0 s. Following 150 µl dH_2O, platelet-rich thrombi (white arrowheads) sequestered in the pulmonary arteriole (t = 10 s). By t = 15 s, the thrombi were trapped in the arteriolar bottlenecks causing local impairments in blood flow. Pulmonary thrombosis started to resolve by t = 23 s and completely resolved by t = 2 min. Data representative of seven independent experiments. Platelets are shown in green and pulmonary microcirculation in purple. * denote alveoli. Dotted ellipses denote arteriolar bottlenecks. White arrow marks the direction of blood flow within the feeding arteriole. The diameter of the shown

arteriole is 29 μm. Scale bar 50 μm. Complete qFILM time series corresponding to panel A is shown in Supplemental Video 2. **(B)** Pulmonary thrombi area plotted as a function of time showing changes in the total area of platelet-rich thrombi following 150 μl IV dH_2O. Red arrow indicates pulmonary thrombi max area.

Figure 2

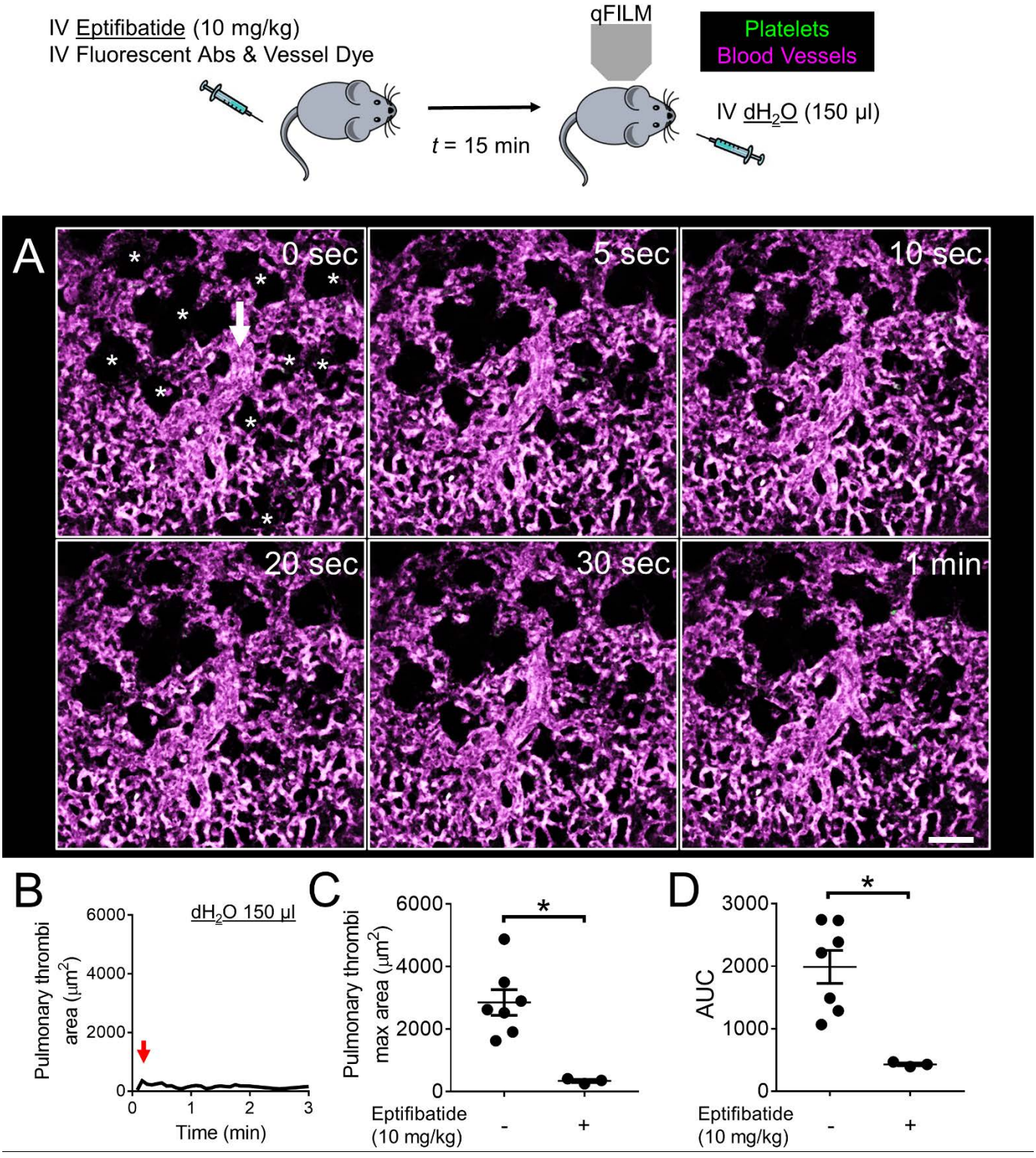
IV Eptifibatide (10 mg/kg)
IV Fluorescent Abs & Vessel Dye
qFILM
Platelets
Blood Vessels
t = 15 min
IV dH2O (150 µl)
A
0 sec
5 sec
10 sec
20 sec
30 sec
1 min
B
dH2O 150 µl
Pulmonary thrombi area (µm2)
Time (min)
C
Pulmonary thrombi max area (µm2)
Eptifibatide (10 mg/kg)
D
AUC
Eptifibatide (10 mg/kg)

Figure 2. Acute hemolysis-induced pulmonary thrombosis is αIIbβ3-dependent. WT mice were intravascularly (IV) administrated with 150 µl dH_2O to trigger acute hemolysis with or without IV administration of 10 mg/kg αIIbβ3-inhibitor (eptifibatide) 15 minutes before IV dH_2O. Pulmonary circulation was imaged using quantitative fluorescence intravital lung microscopy (qFILM). Refer to experimental scheme shown on top. **(A)** qFILM images of the same field of view (FOV) at 6 different time points are shown to assess the effect of 10 mg/kg IV eptifibatide on the development of 150 µl IV dH_2O-dependent pulmonary thrombosis. t = 0 s corresponds to time point before and t > 0 s correspond to time points immediately following IV dH_2O administration. Pulmonary thrombosis was absent at t = 0 s. dH_2O failed to evoke pulmonary thrombosis in mouse pretreated with eptifibatide. Platelets (green) and pulmonary microcirculation (purple). * denote alveoli. White arrow mark the direction of blood flow within the feeding arteriole. The diameter of the shown arteriole is 30 µm. Scale bar 50 µm. Also refer to Supplemental Video 3. **(B)** Pulmonary thrombi area plotted as a function of time for the FOV shown in panel A. Red arrow indicates pulmonary thrombi maximum area (Pulmonary thrombi max area). **(C)** Pulmonary thrombi max area and **(D)** area under the curve (AUC) in mice with (n = 3 mice) or without (n = 7 mice) pretreatment with 10 mg/kg IV eptifibatide prior to 150 µl IV dH_2O. Pulmonary thrombi max area and AUC were estimated as described in Methods. Pulmonary thrombi max area and AUC were compared using Wilcoxon-Mann-Whitney test. Data represent mean ± SE. *P<0.05 when comparing with and without 10 mg/kg IV eptifibatide pretreatment.

Figure 3

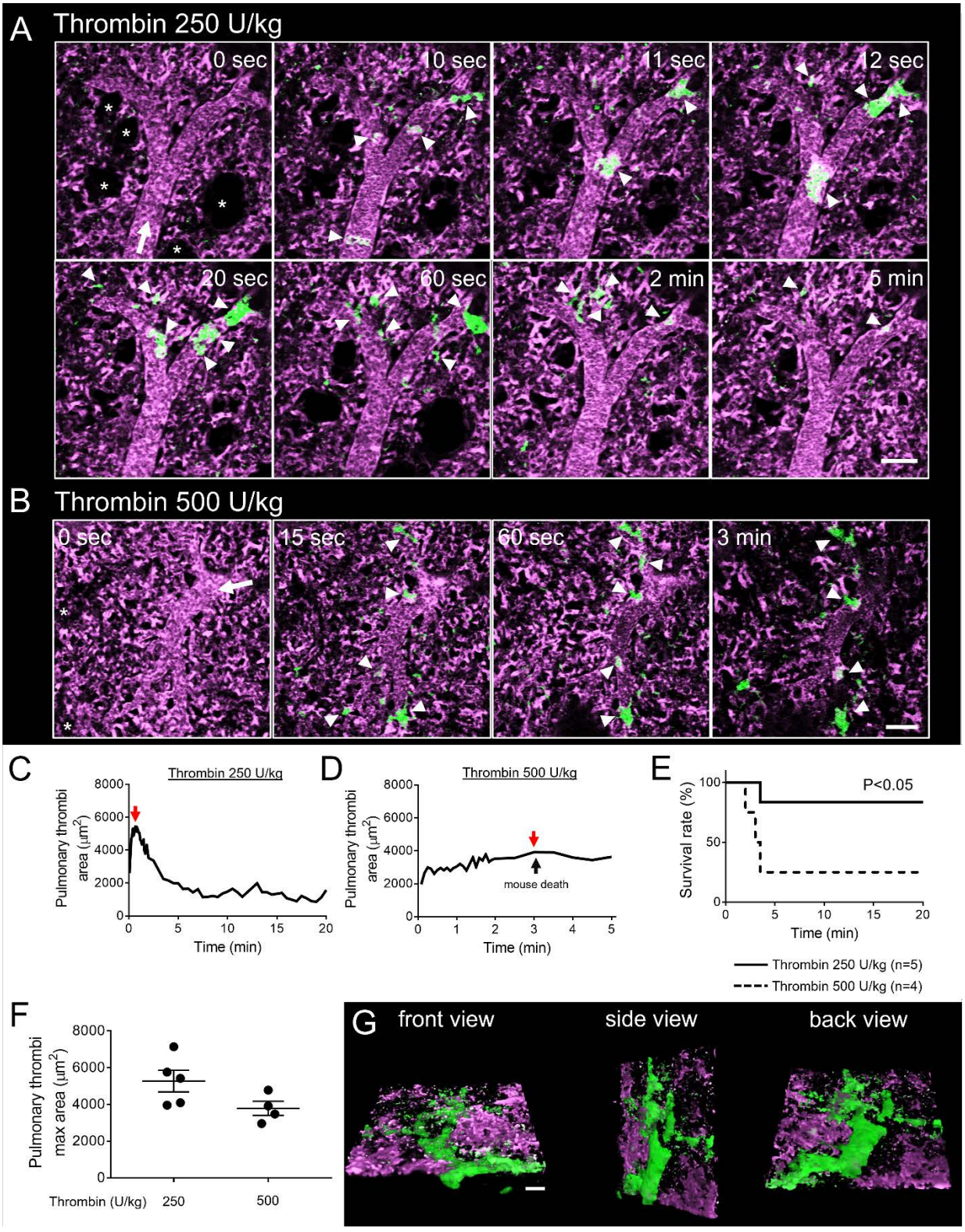
A
Thrombin 250 U/kg
0 sec
10 sec
11 sec
2 sec
20 sec
60 sec
2 min
5 min
B
Thrombin 500 U/kg
0 sec
15 sec
60 sec
3 min
C
Thrombin 250 U/kg
Pulmonary thrombi area (μm²)
Time (min)
D
Thrombin 500 U/kg
mouse death
Pulmonary thrombi area (μm²)
Time (min)
E
P<0.05
Survival rate (%)
Time (min)
Thrombin 250 U/kg (n=5)
Thrombin 500 U/kg (n=4)
F
Pulmonary thrombi max area (μm²)
Thrombin (U/kg)
250
500
G
front view
side view
back view

Figure 3. Thrombin triggers protracted and lethal pulmonary thrombosis in mice. WT mice were administered IV with 250 U/kg (n = 5 mice) or 500 U/kg (n = 4 mice) thrombin and pulmonary circulation was imaged using qFILM. **(A, B)** qFILM images of the same FOV at different time points are shown. t = 0 s corresponds to time point before and t > 0 s correspond to time points following IV thrombin administration. Pulmonary thrombosis was absent at t = 0 s. Platelets are shown in green and pulmonary microcirculation in purple. **(A)** Following 250 U/kg IV thrombin, small (<500 μm^2) and medium (500-1000 μm^2) platelet-rich thrombi (white arrowheads) sequestered in the pulmonary arteriole (t = 10 to 12 s) and obstructed blood flow (t = 20 s). **(B)** Following 500 U/kg IV thrombin, small (<500 μm^2) and medium (500-1000 μm^2) platelet-rich thrombi (white arrowheads) sequestered in the pulmonary arteriole to occlude the arteriolar bottlenecks. The mouse died by t = 3 min leading to arrest of pulmonary blood flow, which was evident by the reduced intensity of vascular dye (purple fluorescence), and stationary erythrocytes (refer to Supplemental Video 5). * denote alveoli. White arrows mark the direction of blood flow. The diameters of the arterioles shown in A and B are 39 μm and 44 μm, respectively. Complete qFILM time series corresponding to panels A and B shown in Supplemental Videos 4 and 5, respectively. **(C, D)** Pulmonary thrombi area plotted as a function of time following 250 U/kg **(C)** and 500 U/kg **(D)** IV thrombin within FOVs shown in panels A and B, respectively. Red and black arrows indicate pulmonary thrombi maximum area (Pulmonary thrombi max area) values and the time of mouse death following 500 U/kg IV thrombin, respectively. **(E)** Survival rate during qFILM experiments in WT mice IV administered with either 250 U/kg (n = 5 mice) or 500 U/kg (n = 4) thrombin (p = 0.046, log-rank test). **(F)** Pulmonary thrombi max areas in mice following 250 U/kg (n = 5 mice) and 500 U/kg (n = 4 mice) IV thrombin. Pulmonary thrombi max areas were compared using Wilcoxon-Mann-Whitney test. Data represent mean ± SE. **(G)** Three-

Dimensional qFILM image of a lethal pulmonary thrombosis developed within a large pulmonary arteriole (57 μm) of a mouse administered with 500 U/kg IV thrombin. Platelets (green) and pulmonary microcirculation (purple). Refer to Supplemental Video 6. Scale bar 50 μm.

Figure 4

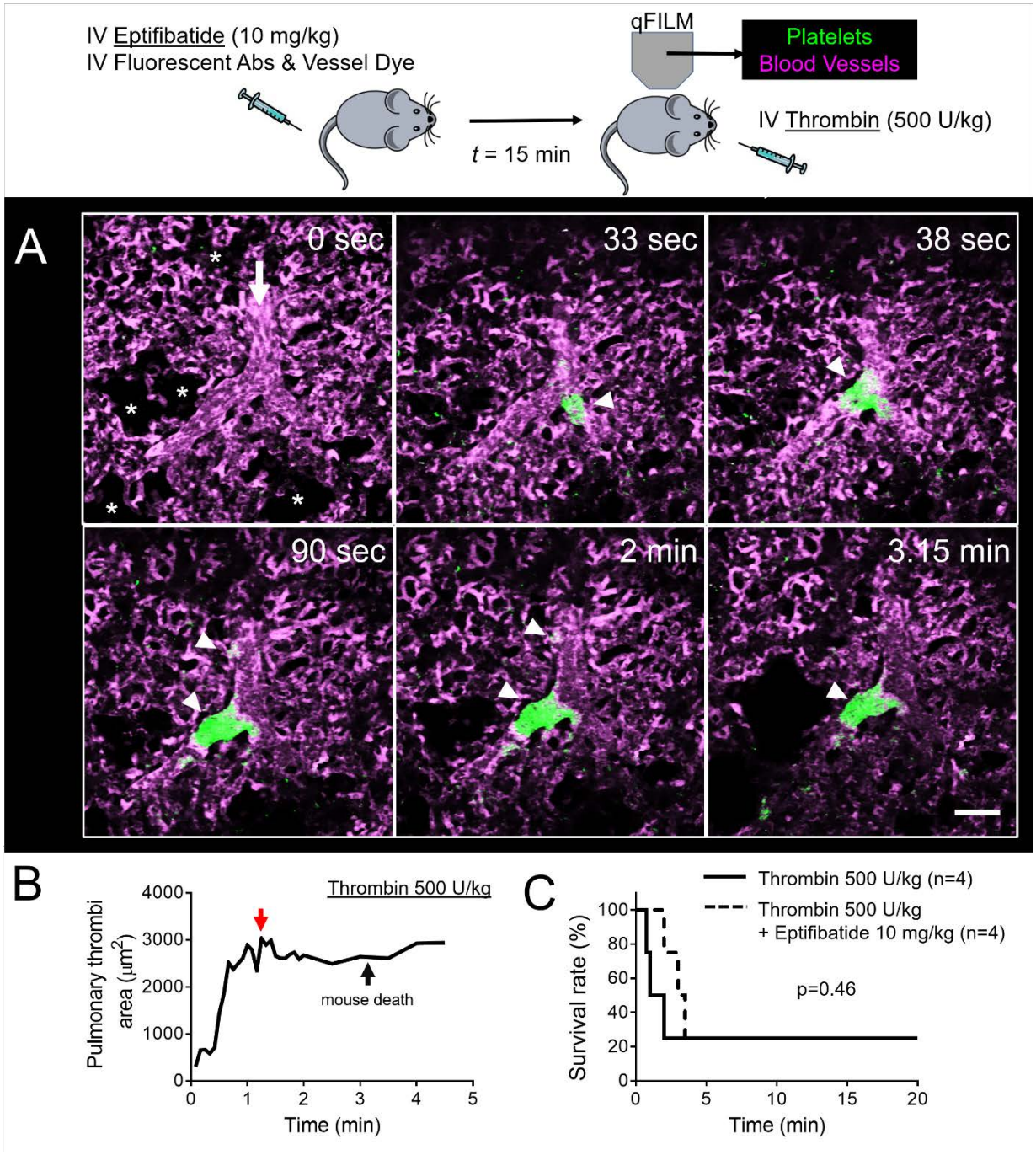

Figure 4. Thrombin-triggered lethal pulmonary thrombosis is platelet-αIIbβ3 independent. WT mice were intravascularly (IV) administered 500 U/kg thrombin with or without IV administration of 10 mg/kg αIIbβ3-inhibitor (eptifibatide) 15 minutes before IV thrombin.

Pulmonary circulation was imaged using quantitative fluorescence intravital lung microscopy (qFILM). Refer to experimental scheme shown on top. **(A)** qFILM images of the same field of view (FOV) at 6 different time points are shown to assess the effect of 10 mg/kg IV eptifibatide on the development of 500 U/kg IV thrombin-dependent pulmonary thrombosis. t = 0 s corresponds to time point before and t > 0 s correspond to time points immediately following IV thrombin administration. Pulmonary thrombosis was absent at t = 0 s. Following 500 U/kg IV thrombin, medium (500-1000 μm^2) and large (>1000 μm^2) platelet-rich thrombi (white arrowheads) sequestered in the pulmonary arteriole and traveled down the pulmonary arterioles to occlude the arteriolar bottlenecks (t = 90 s). Mouse died at t = 3.15 min leading to arrest of pulmonary blood flow, which was evident by the presence of stationary erythrocytes (Supplemental Video 7) and decrease in vascular dye (purple fluorescence) in the FOV. Platelets (green) and pulmonary microcirculation (purple). * denote the alveoli. White arrow marks the direction of blood flow. The diameter of the arteriole is 33 μm. Scale bar 50 μm. See also Supplemental Video 7 for the complete qFILM time series. **(B)** Pulmonary thrombi area plotted as a function of time for the FOV shown in panel A. Red and black arrows indicate pulmonary thrombi maximum area (Pulmonary thrombi max area) and the time of mouse death, respectively. **(C)** Survival rate during qFILM experiments in WT mice pretreated (n = 4 mice) or untreated (n = 4 mice) with 10 mg/kg IV eptifibatide prior to 500 U/kg IV thrombin (p = 0.46, log-rank test).

Figure 5

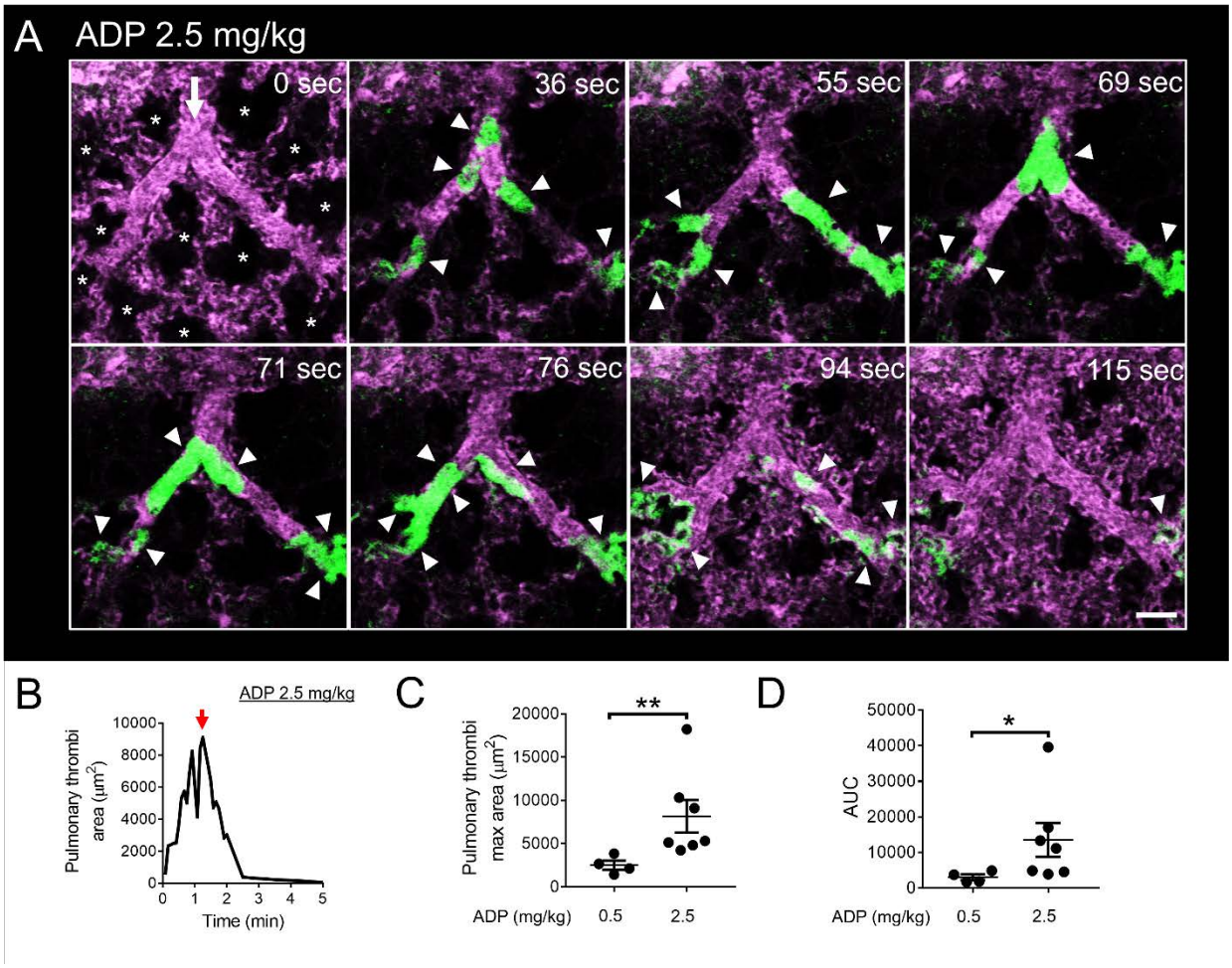

Figure 5. ADP triggers reversible acute pulmonary thrombosis in mice. WT mice were intravascularly (IV) administered either 0.5 mg/kg ADP (n = 4 mice) or 2.5 mg/kg ADP (n = 7 mice) and pulmonary circulation was imaged using quantitative fluorescence intravital lung microscopy (qFILM). **(A)** qFILM images of the same field of view (FOV) at 8 different time points are shown. t = 0 s corresponds to time point before IV ADP administration and other displayed time points are relative to IV ADP. Pulmonary thrombosis was absent at t = 0 s. Following 2.5 mg/kg IV ADP, medium (500-1000 μm^2) and large size (>1000 μm^2) platelet-rich thrombi (white arrowheads) sequestered in the pulmonary arteriole (t = 36 s). The thrombi obstructed the arteriolar bottlenecks (t = 55 s) resulting in loss of the pulmonary blood flow, which was evident by the

absence of the vascular dye (purple fluorescence) in the capillaries downstream of the embolized arteriole. Pulmonary thrombosis resolved and the capillary blood flow recovered (purple fluorescence was back) by t = 115 s. Platelets (green) and pulmonary microcirculation (purple). * denote alveoli. White arrows mark the direction of blood flow. The diameters of the arteriole shown in A is 41 μm. Scale bar 50 μm. Complete qFILM time series corresponding to panels A is shown in Supplemental Video 9. **(B)** Pulmonary thrombi area plotted as a function of time to show changes in the total area of platelet-rich thrombi following 2.5 mg/kg IV ADP within FOV shown in panel A. Pulmonary thrombi maximum area (Pulmonary thrombi max area) value marked by red arrow. **(C)** Pulmonary thrombi max area and **(D)** area under the curve (AUC) were estimated to compare pulmonary thrombosis development in mice following 0.5 mg/kg IV ADP (n = 4 mice) and 2.5 mg/kg IV ADP (n = 7 mice). Pulmonary thrombi max area and AUC were compared using Wilcoxon-Mann-Whitney test. Data represent mean ± SE. *P < 0.05, **P<0.01 for 0.5 mg/kg vs. 2.5 mg/kg IV ADP.

Figure 6

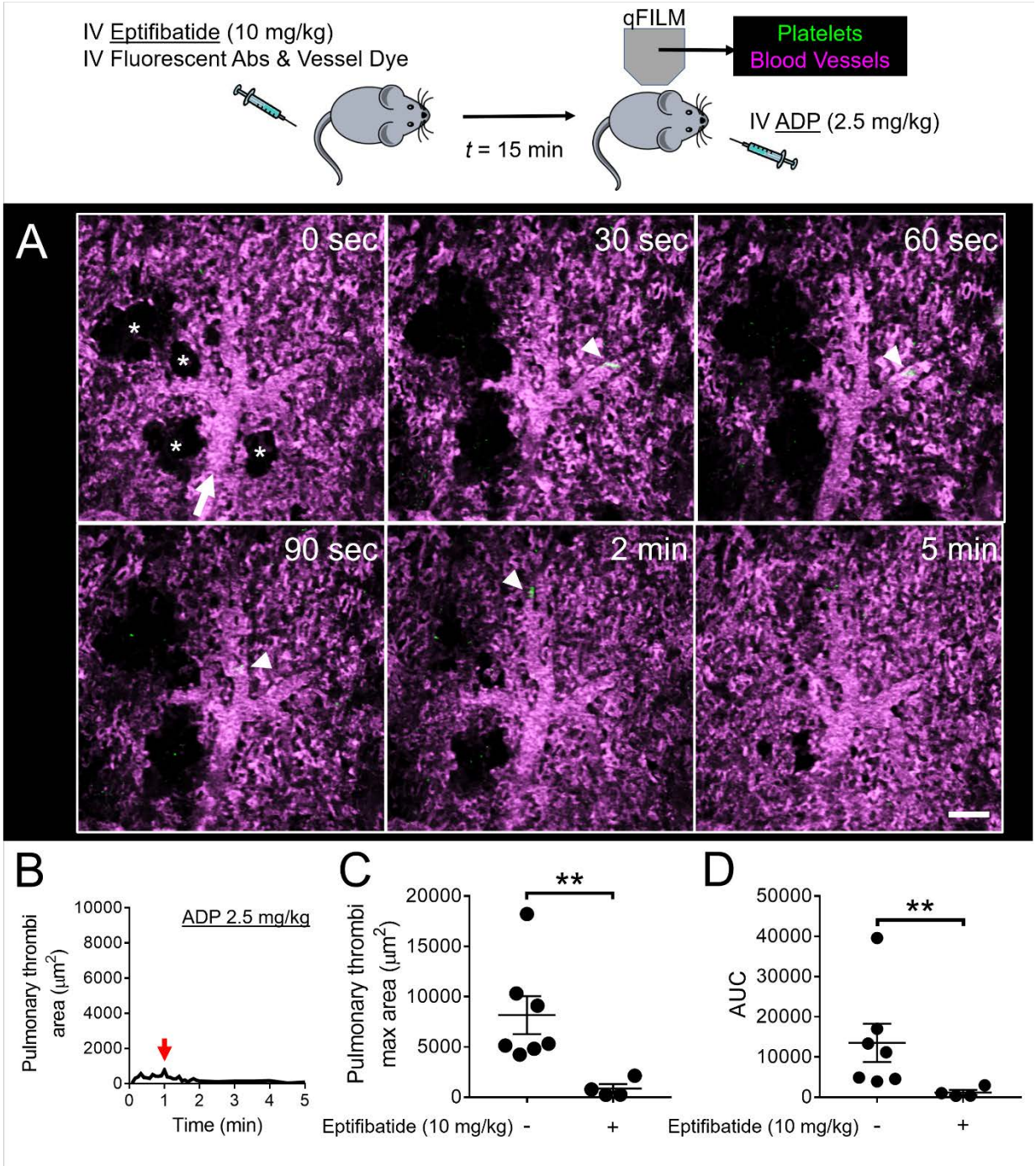

Figure 6. ADP-induced pulmonary thrombosis in mice is αIIbβ3-dependent. WT mice were intravascularly (IV) administered 2.5 mg/kg ADP with or without IV administration of 10 mg/kg αIIbβ3-inhibitor (eptifibatide) 15 minutes before IV ADP. Pulmonary circulation was imaged using

quantitative fluorescence intravital lung microscopy (qFILM). Refer to experimental scheme shown on top. **(A)** qFILM images of the same field of view (FOV) at 6 different time points are shown to assess the effect of eptifibatide on the development of IV ADP-dependent pulmonary thrombosis. t = 0 s corresponds to time point before and t > 0 s correspond to time points immediately following IV ADP administration. Pulmonary thrombosis was absent at t = 0 s. ADP failed to evoke pulmonary thrombosis in mouse pretreated with eptifibatide. Platelets (green) and pulmonary microcirculation (purple). * denote alveoli. White arrows mark the direction of blood flow within the arterioles. The diameter of the arteriole shown is 38 μm. Scale bar 50 μm. **(B)** Pulmonary thrombi area plotted as a function of time for the FOV shown in panel A. Red arrow indicates pulmonary thrombi maximum area (Pulmonary thrombi max area). **(C)** Pulmonary thrombi max area and **(D)** area under the curve (AUC) in mice with (n = 4 mice) or without (n = 7 mice) pretreatment with eptifibatide prior to IV ADP. Pulmonary thrombi max area and AUC were estimated as described in Methods. Pulmonary thrombi max area and AUC were compared using Wilcoxon-Mann-Whitney test. Data represent mean ± SE. **P<0.01 when comparing with and without eptifibatide pretreatment.

Figure 7

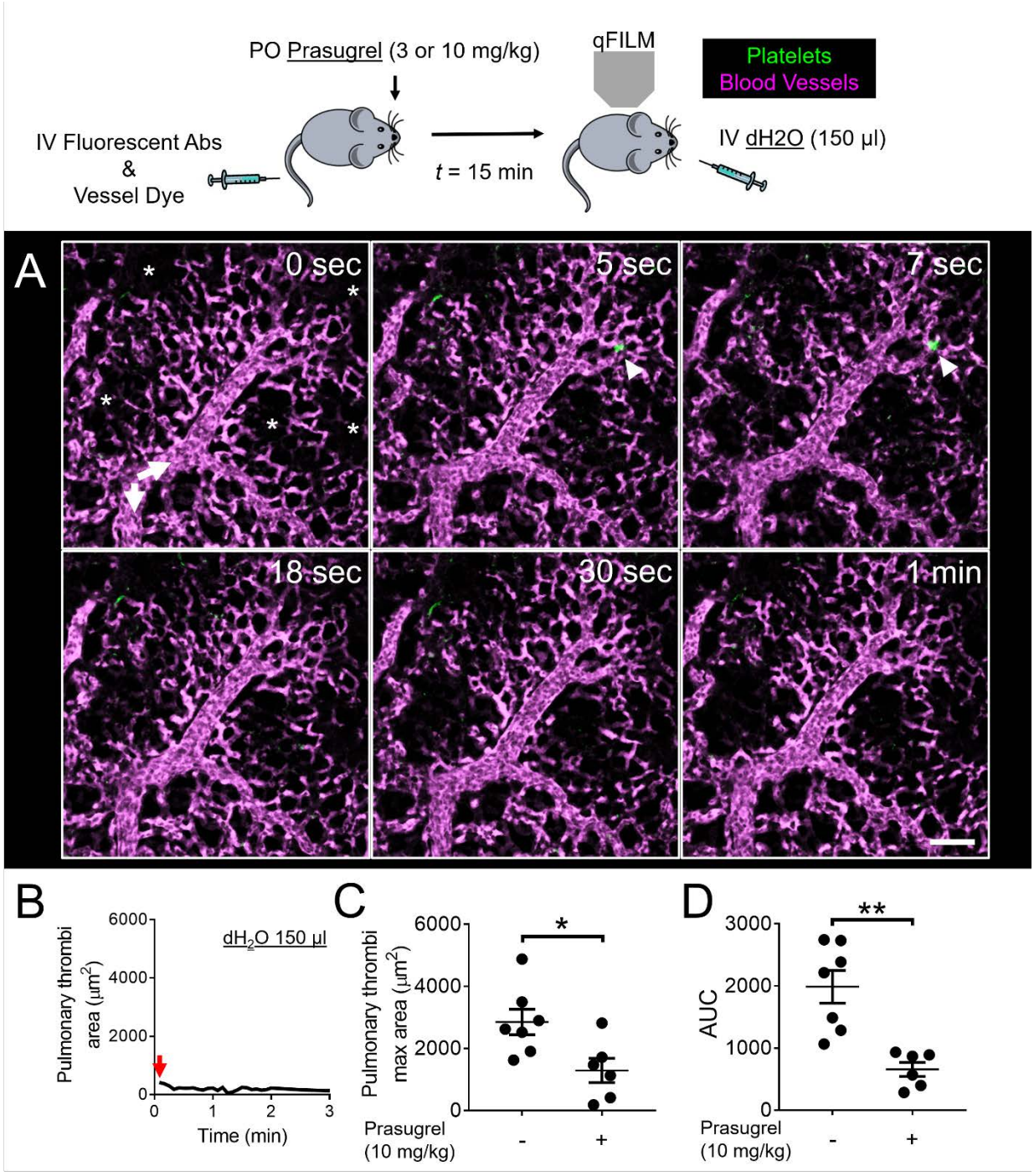

Figure 7. Inhibition of platelet $P2Y_{12}$-receptor abrogates hemolysis-induced pulmonary thrombosis in mice. WT mice were administered 10 mg/kg prasugrel by oral gavage (for more

details refer to Methods) and then intravascularly (IV) challenged with 150 µl dH_2O. Refer to schematic on top. Pulmonary circulation was imaged using quantitative fluorescence intravital lung microscopy (qFILM). **(A)** qFILM images of the same field of view (FOV) at 6 different time points are shown. t = 0 s corresponds to time point before and t > 0 s correspond to time points immediately following IV dH_2O administration. Pulmonary thrombosis was absent at t = 0 s. dH_2O failed to evoke pulmonary thrombosis in mouse pretreated with prasugrel. Platelets (green) and pulmonary microcirculation (purple). * denote alveoli. White arrows mark the direction of blood flow within the feeding arterioles. The diameter of the arteriole shown is 30 µm. Scale bar 50 µm. Also refer to Supplemental Video 11. **(B)** Pulmonary thrombi area plotted as a function of time for the FOV shown in panel A. Red arrow indicates pulmonary thrombi maximum area (Pulmonary thrombi max area). **(C)** Pulmonary thrombi max area and **(D)** area under the curve (AUC) in mice with (n = 6 mice) or without (n = 7 mice) pretreatment with prasugrel prior to IV dH_2O. Pulmonary thrombi max area and AUC were estimated as described in Methods. Pulmonary thrombi max area and AUC were compared using Wilcoxon-Mann-Whitney test. Data represent mean ± SE. *P < 0.05, **P<0.01 when comparing with and without prasugrel pretreatment.